zyme structure can have profound effects on the ability of an enzyme to function effectively.

The A3, A34, A58, A78, A85, and A89 proteins appear to have retained both the unusual wild-type conformation in the sulfhydryl-group region as well as the ability to bind substrate. It should be pointed out, however, that these treated proteins were not further characterized to determine whether NEM had reacted with the cysteine residues in the same fashion as in the normal enzyme, although this does seem likely.

Ignoring this reservation one would conclude that alteration of some property other than the conformation in the cysteine-containing region and the ability to bind substrate is responsible for their lack of enzymatic activity or that the methods used are not sufficiently sensitive to detect subtle, yet critical, changes. There is the possibility, for example, that these methods cannot detect "proper" substrate binding, which may involve specific and additional associations required for substrate turnover that are not possible with the mutant proteins.

The mutant A proteins from A46 and A23, on the other hand, do show marked differences in behavior from the wild-type enzyme. Both mutant proteins appear to lack the ability to bind InGP at the cysteine-containing region. Although these proteins do have charge differences from the normal enzyme (Fig. 1), this fact alone could not explain their behavior since three of the other mutant proteins, A3, A34, and A58, also have charge changes and are similar to the normal enzyme in substrate-binding properties. However, the A46-A23 site in the protein may be more critically involved in maintaining a proper conformation for InGP binding than some other regions of the polypeptide chain and thus a charge change here may have a more severe effect. The finding with A46 and A23 revertant proteins (containing either a valine or isoleucine residue in place of a charged residue) that there is concomitant restoration of enzymatic activity and substrate-binding ability supports this view.

JOHN K. HARDMAN
McCollum-Pratt Institute, Biology Department, Johns Hopkins University, Baltimore, Maryland
CHARLES YANOFSKY
Department of Biological Sciences, Stanford University, Stanford, California

References and Notes

1. D. R. Helinski and C. Yanofsky, *Proc. Nat. Acad. Sci. U.S.* **48**, 173 (1962); U. Henning and C. Yanofsky, *ibid.* pp. 183 and 497; D. R. Helinski and C. Yanofsky, *J. Biol. Chem.* **238**, 1043 (1963); J. R. Guest and C. Yanofsky, *ibid.* **240**, 679 (1965); B. C. Carlton and C. Yanofsky, *ibid.*, p. 690.
2. J. K. Hardman and C. Yanofsky, *J. Biol. Chem.* **240**, 725 (1965).
3. C. Yanofsky, G. R. Drapeau, J. R. Guest, B. C. Carlton, *Proc. Nat. Acad. Sci. U.S.* **57**, 296 (1967).
4. R. D. Hotchkiss and A. H. Evans, *Fed. Proc.* **19**, 912 (1960); A. M. Albrecht, J. L. Palmer, D. J. Hutchinson, *J. Biol. Chem.* **241**, 1043 (1966).
5. M. J. Schlesinger, *J. Biol. Chem.* **241**, 3181 (1966).
6. Supported by grants from USPHS and NSF. We thank Virginia Horn, D. Vinicor, and Deanna Thorpe for technical assistance.

20 April 1967

Yeast Transfer RNA: A Small-Angle X-Ray Study

Abstract. *The intensity of x-ray scattering and the radius of gyration were measured for a mixture of yeast transfer RNA's in tenth molar potassium chloride. The experimentally observed radius of gyration eliminates single-stranded, hairpin, singly folded hairpin, triple-stranded, and linked double-hairpin models of tRNA but allows certain folded cloverleaf models. The measured intensities at larger angles, beyond the radius of gyration region, lend some support to the Holley's cloverleaf model, in which three arms are folded up tightly together and the fourth arm is extended in the opposite direction.*

The base sequences are known (*1*, *2*) for several transfer RNA's (tRNA) from yeast, and there have been a number of suggestions of possible base pairings and molecular conformations. However, the molecule has not been crystallized, and the tertiary structure is not known. We have measured the x-ray scattering from dilute solutions of tRNA and have calculated the scattering expected from several arrangements of Holley's (*1*) cloverleaf model of the molecule. Most of the more open or extended tertiary structures are unlikely.

Measurements of x-ray scattering at small angles were made upon a mixture of yeast transfer RNA's in 0.1*M* KCl, 0.02*M* tris (hydroxymethyl) aminomethane-hydrochloride buffer at *p*H 7.42. The x-ray data were corrected simultaneously for effects due to slit height and width (*3*). The radius of gyration, *Rg*, was found to be 23.5 Å ± .25 Å, and the weight-average molecular weight, as determined from the absolute forward scattering, was 27,500. The x-ray scattered intensities in the shape region (that is, the region from 10 to 70 milliradians for tRNA, see Fig. 2) do not agree well with the scattering calculated from simple shapes, such as ellipsoids of revolution and cylinders. Radii of gyration for mixtures of yeast tRNA have been published by Krigbaum and Godwin (*4*) (Rg = 23.9 Å) and Dembo, Sosfenov, and Feigin (*5*) (Rg = 21 Å), both values being in reasonable agreement with ours.

The tRNA was prepared by a slight modification of Holley's method (*6*). After chromatographic fractionation of the tRNA (*7*), it was found that the mixture consisted mainly of six tRNA's and included alanine tRNA. The tRNA was then precipitated with ethanol and dried at 4°C over phosphorus pentoxide. At the end of 2 days it was dissolved in 0.1*M* KCl containing 0.02*M* tris-HCl, at *p*H 7.42, and a small amount was chromatographed on Sephadex G-100. The column gave a sharp, symmetrical peak without evidence of dimer or degradation products.

The most striking experimental result is the small radius of gyration. The radius of gyration is measured from the curve of scattered x-ray intensity in the region from 8 to 10 milliradians for tRNA (see Fig. 2) and is defined by

$$(Rg)^2 = (\Sigma\, n_i \cdot r_i^2)/(\Sigma\, n_i)$$

The number of electrons in the ith atom is n_i; r_i is the distance of the ith atom from the center of charge of the molecule, and the sum is over all atoms of the molecule. The experimental radius of gyration may be used to eliminate several tertiary structures which have been suggested. The calculated radius of gyration (28 to 30Å) of the random coil of a single-stranded model is too large. A hairpin model of the tRNA has a radius of gyration of about 40 Å and thus is certainly eliminated, while the same hairpin model folded back upon itself at the middle still has too large a radius of gyration (about 25 Å). A triple-stranded model (*8*) also has too large a radius of gyration (about 28 Å). The model consisting of two linked hairpin regions (*1*) has a radius of gyration of about 25 Å and is probably eliminated. Of the configurations suggested by others, only certain folded Holley cloverleaf models appear to have radii

of gyration which are in the correct range.

The various tRNA molecules are thought to have similar tertiary structures because each must interact with similarly spaced messenger RNA codons, the same ribosome surfaces, and the polypeptide synthetase enzyme. They are reported to have identical molecular weights (*9*) [although some variations have now been shown (*1, 2*)], similar primary and secondary structures (*1, 2*), and similar small-angle x-ray scattering properties (*4*). Thus the cloverleaf model of one tRNA of known base sequence, yeast alanine tRNA, is assumed to be a model for the general features of tRNA. We limit this discussion to cloverleaf models of the known base sequence of alanine tRNA. Since the x-ray data do not extend to atomic resolutions, it was felt adequate, for the calculations, to determine only the coordinates of the centers of electron density of the base, phosphate, and sugar groups. These coordinates were obtained by building Corey-Pauling-Koltun models (*10*) of these regions, photographing the models, and measuring the coordinates from the photographs. In the base-paired regions, a helix with ten base pairs per turn and with 3 Å between each pair was used (*11*). In the nonpaired loops, the bases were folded in a base-stacked single strand to give minimum exposure of hydrophobic surfaces to the solvent. This folding, referred to as "folding in," brings the ribose phosphate chain to the exterior of the loop. In the two loops containing seven bases, it is sterically impossible to "fold in" simultaneously all seven bases. Thus the anticodon, containing the nucleotide triplet IGC (inosinic acid, guanylic acid, cytidylic acid), was not "folded in" and a corresponding nucleotide triplet CGA (cytidylic acid, guanylic acid, adenylic acid) in the remaining loop containing seven bases also was not "folded in." If none of the bases in the loops is "folded in" the calculated radius of gyration is increased by about 2 Å.

In Fig. 1 are shown calculated radii of gyration as functions of the symmetrical opening angle of all four arms. Zero degree corresponds to the planar structure, and 90° corresponds to the axes of the helical regions of each of the four arms folded up parallel to each other and to a normal to the original planar structure. End-group analyses show that the sample is about 90 percent intact and the remainder has the A missing. Thus we expect that the appropriate curve will lie near the solid line. It is concluded from these data that the configuration in which the arms are all oriented at about 60° is a possible structure. The radius of

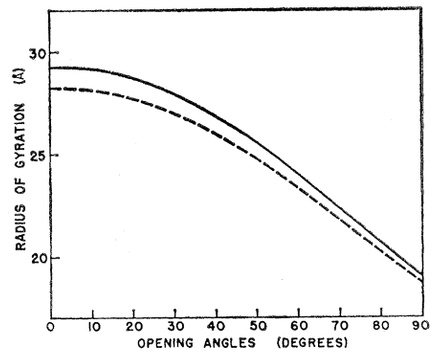

Fig. 1. Calculated radii of gyration are plotted as functions of symmetrical opening angles for various foldings of the arms of a Holley cloverleaf model of alanine tRNA. The solid line is the radius of gyration of the molecule with the C-C-A end group attached, while the dashed line represents the radius of gyration of the molecule with the C-C-A end group removed.

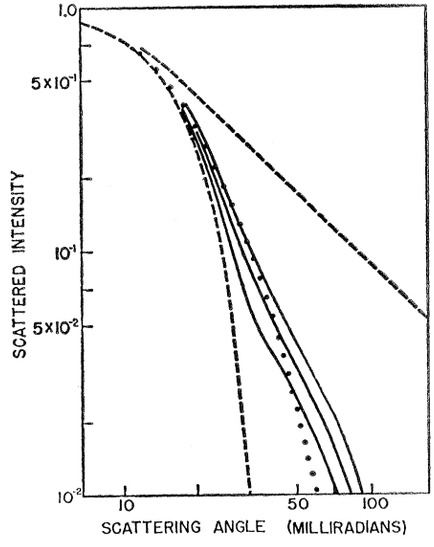

Fig. 2. The experimental intensity of x-ray scattering at angles beyond the radius of gyration region is compared with various theoretical curves. All curves are scaled to a common radius of gyration of 23.5 Å. The upper and lower dashed curves are the scatterings predicted from an infinitely long right circular cylinder of uniform electron density and a sphere of uniform electron density, respectively. They are for comparison and represent the extremes which the scattered intensity may assume. The three solid lines are, from top to bottom, the scattering from Holley cloverleaf models of alanine tRNA in which all the arms are oriented at angles of 30°, 50°, and 70° with respect to the plane defined by the model in its most extended conformation. The experimentally measured points are shown as solid dots. The x-ray wavelength is 1.54 Å.

gyration measurement is equally consistent with a distribution of conformations averaging around 60°.

In Fig. 2 the scattering at larger angles, calculated from the model, is compared to the observations. Down to about 0.07 of the central intensity the scattering from the 30° model and the experimental curve agree quite well, but this model is excluded by the radius of gyration. At larger scattering angles the calculated scattering from various arrangements of the arms, including a number of unsymmetrical arrangements, exhibits a shoulder in the region of 60 milliradians (corresponding to a Bragg spacing of 26 Å) which is not present in the experimental curve. This shoulder at 60 milliradians has its physical origin in the interference of the scattered x-rays from the different arms of the cloverleaf. Presumably, a configuration in which the arms are not "discrete," but are folded tightly together to form a single unit, would not have this shoulder. The scattered intensity from a configuration in which three arms are positioned closely together, and the fourth arm (possibly containing the anticodon) is extended in the opposite direction, should not have a 60-milliradian shoulder. The radius of gyration of this model is about 23 Å and the height-to-diameter ratio is between 2 and 2.5. Both of these values are in general agreement with the experimentally observed curve in the radius of gyration region and in the shape region. Detailed calculations to test such a model would be time consuming and have not yet been attempted.

In conclusion, it appears that yeast tRNA must have a rather compact structure. A single-stranded model, a triple-stranded model, and various hairpin models are inconsistent with the x-ray data. A Holley cloverleaf structure may be folded to have the compactness required by the observed radius of gyration. The Holley cloverleaf model in which three arms are folded up tightly together, and the fourth arm is extended in the opposite direction, seems to be in agreement with the experimentally observed radius of gyration and the x-ray scattering which is observed at larger angles.

Note added in proof: Since this manuscript was submitted we have calculated the scattering to be expected from Holley models in which some of the arms are placed in close side-by-side contact. As surmised in the text above, the troublesome shoulder near

60 milliradians is almost eliminated, and the agreement with experiment is considerably improved. However, the recent calculations indicate that a Holley model—with two arms in close contact, pointing up, and the other two in close contact and pointing down—is in satisfactory agreement with our measurements. Thus the x-ray data alone do not distinguish between this model and the three-up and one-down model suggested in the text.

J. A. LAKE
W. W. BEEMAN
Biophysics Laboratory,
University of Wisconsin, Madison 53706

References and Notes

1. R. Holley, J. Apgar, G. Everett, J. Madison, M. Marquisee, S. Merrill, J. Penwick, A. Zamir, *Science* **147,** 1462 (1965).
2. J. Madison, G. Everett, H. Kung, *ibid.* **153** 531 (1966); H. Zachau, D. Dutting, H. Feldman, *Angew. Chem.* **78,** 392 (1966); U. RajBhandary, S. Chang, A. Stuart, R. Faulkner, R. Hoskinson, H. Khorana, *Proc. Nat. Acad. Sci. U.S.* **57,** 751 (1967).
3. J. Lake, *Acta Cryst.*, in press.
4. W. Krigbaum and R. Godwin, *Science* **154,** 423 (1966).
5. A. Dembo, N. Sosfenov, L. Feigin, *Kristallagrafiya* **11,** 581 (1966).
6. R. Holley, *Biochem. Biophys. Res. Commun.* **10,** 186 (1963).
7. J. Cherayil and R. Bock, *Biochemistry* **4,** 1174 (1965).
8. W. Guschlbauer, *Nature* **209,** 258 (1966).
9. T. Lindahl, D. Henley, J. Fresco, *J. Amer. Chem. Soc.* **87,** 4961 (1965).
10. W. Koltun, *Biopolymers* **3,** 665 (1965).
11. K. Tomita and A. Rich, *Nature* **201,** 1160 (1964).
12. We thank Professor Robert Bock for his generous gift of yeast tRNA. I thank Professor Bock, Professor J. Anderegg, A. Hampel, and L. Kirkegaard for advice and assistance in the handling of the tRNA and in the interpretation of results. Supported by research and training grants from NIH and a predoctoral fellowship from NSF.

3 March 1967

Lepidocrocite, an Apatite Mineral, and Magnetite in Teeth of Chitons (Polyplacophora)

Abstract. *X-ray diffraction patterns show that the mature denticles of three extant chiton species are composed of the mineral lepidocrocite and an apatite mineral, probably francolite, in addition to magnetite. Each of the three minerals forms a discrete microarchitectural unit of the chiton denticles. This is the first indication that lepidocrocite is precipitated by marine organisms and an apatite mineral by chitons.*

Occurrences of magnetite ($Fe_2O_3 \cdot FeO$) in marine sediments have been attributed in the past to volcanic sources or were thought to be derived from cosmic spherules. However, this mineral is also a biological precipitate (*1*). The organisms now known to synthesize magnetite are chitons, which are common in the intertidal zone of rocky shores on the continents and oceanic islands, while a few species are known to occupy ocean deeps up to 4200 m (*2*). Magnetite in chitons is localized in the mineralized denticles of the mature major lateral teeth; the identification of the mineral is based on study of denticle samples by x-ray diffraction, on determination of the ferric-ferrous ration, and on the hardness on the Mohs hardness scale (*1, 3*). Denticles from ten species of chitons were investigated, and magnetite was found in all cases (*1, 4*). However, the x-ray diffraction photographs for a number of chiton species showed not only the magnetite pattern but, in addition, several weak lines (*1*). These additional lines indicated the presence of other minerals which could be either goethite, lepidocrocite, or carbonate apatite, or a combination thereof (*1*).

In mollusca, the mineral goethite (αFeOOH) is known to occur in the mineralized denticles of one gastropod family (*5*), and dahllite possibly occurs in the larval shells of one bivalve species (*6*). There is no reliable record of lepidocrocite (γFeOOH) as a biologic mineral precipitate. Hence, it is important to define these unidentified minerals that occur in some chiton teeth and to determine their distribution relative to the magnetite in the mineralized denticles.

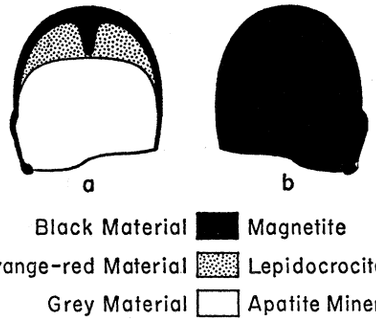

Fig. 1. Distribution of the three microarchitectural units on the denticle surfaces of the teeth of *Acanthopleura echinatum*. (a) Anterior surface view; (b) posterior surface view. Denticle dimensions: height and width, 0.7 mm.

We selected species of the Chitonidae for the study, because three of the species that indicated unidentified minerals in addition to magnetite belong to the genera *Chiton* and *Acanthopleura* from this family. The denticles of mature mineralized teeth (major laterals) were mechanically separated from specimens (preserved in alcohol) of *Chiton tuberculatus* from Barbados, West Indies, of *Acanthopleura echinatum* from Viña del Mar, Chile, and of *A. spiniger* from Fiji and Palau, Caroline Islands (*7*). A sample of entire denticles from each species was examined under the microscope for their surface colors, and thin sections were prepared from another sample to compare the colors of their interiors with those on the surfaces.

The denticles of all three species have several features in common. They are similar in shape, and their surfaces show differently colored regions; one of these regions is characterized by a black shiny material and is always found in a homologous position on the denticle surfaces. Species-defined differences are marked by minor color variations in the area unoccupied by the black material. In *Acanthopleura echinatum*, the remainder of the denticle surface is characterized by two distinct color regions, one with bright orange-red and the other with a light gray color. The distribution and boundary relations of the black, orange-red, and gray materials on the denticle surfaces of *A. echinatum* are shown in Fig. 1.

The region occupied by the bright orange-red material in *A. echinatum*

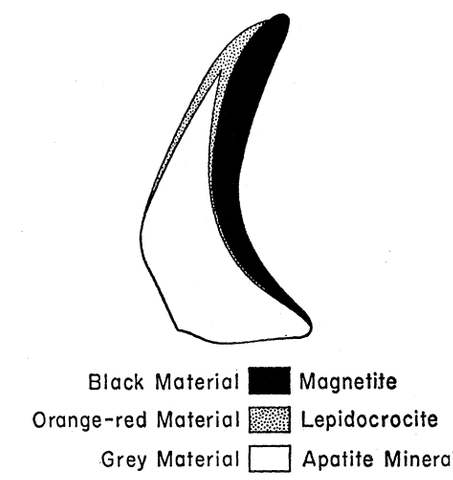

Fig. 2. Distribution of the three microarchitectural units in the inside of the denticles of *A. echinatum*, as seen in the median longitudinal cut through the denticle.